

Vibrations of Jammed Disk Packings with Hertzian Interactions

Carl F. Schreck^{1,2}, Corey S. O'Hern^{1,2,3}, and Mark D. Shattuck^{4,1}

¹*Department of Mechanical Engineering & Materials Science,
Yale University, New Haven, Connecticut 06520-8260, USA*

²*Department of Physics, Yale University, New Haven, Connecticut 06520-8120, USA*

³*Department of Applied Physics, Yale University, New Haven, Connecticut 06520-8120, USA and*

⁴*Benjamin Levich Institute and Physics Department,
The City College of the City University of New York, New York, New York 10031, USA*

Contact breaking and Hertzian interactions between grains can both give rise to nonlinear vibrational response of static granular packings. We perform molecular dynamics simulations at constant energy in 2D of frictionless bidisperse disks that interact via Hertzian spring potentials as a function of energy and measure *directly* the vibrational response from the Fourier transform of the velocity autocorrelation function. We compare the measured vibrational response of static packings near jamming onset to that obtained from the eigenvalues of the dynamical matrix to determine the temperature above which the linear response breaks down. We compare packings that interact via single-sided (purely repulsive) and double-sided Hertzian spring interactions to disentangle the effects of the shape of the potential from contact breaking. Our studies show that while Hertzian interactions lead to weak nonlinearities in the vibrational behavior (e.g. the generation of harmonics of the eigenfrequencies of the dynamical matrix), the vibrational response of static packings with Hertzian contact interactions is dominated by contact breaking as found for systems with repulsive linear spring interactions.

PACS numbers: 63.50.Lm, 63.50.-x, 64.70.pv, 83.80.Fg

I. INTRODUCTION

Dry granular media are composed of discrete grains that interact via purely repulsive, frictional contact interactions. Without external driving, granular materials form static packings that possess nonlinear response to external perturbations [1, 2]. For example, the acoustic response of granular packings includes harmonic mode generation, mixing, attenuation, and dispersion, which have been exploited to engineer novel phononic metamaterials that can act as rectifiers and filters [3]. There are many sources of nonlinearity in granular media, which include 1) the nonlinear form of Hertzian interactions between grains [4], 2) contact breaking and formation (*i.e.* contact clapping [5]) that occurs frequently in systems with purely repulsive contact potentials, and 3) rolling and sliding frictional contacts. In prior studies, we isolated the nonlinearities that arise from contact breaking by measuring the vibrational response of mechanically stable (MS) packings of frictionless disks that interact via purely repulsive linear spring potentials [6, 7]. In this manuscript, we perform computational studies to determine the relative contributions of the nonlinearities that arise from the shape of the Hertzian potential and contact breaking by measuring the vibrational response of MS packings that interact via single- (repulsive only) and double-sided (repulsive and attractive) Hertzian springs.

We find two overarching results: 1) The shape of the Hertzian interaction potential gives rise to nonlinearities in the vibrational response of jammed disk packings, such as the generation of harmonics of the driving frequency and beats among these and normal mode frequencies from the dynamical matrix. 2) However, these nonlinearities are weak compared to those generated by contact breaking in systems with purely repulsive Hertzian spring interactions. In particular, prior to contact breaking (over the timescales we considered), the measured density of vibrational modes for jammed packings with Hertzian interactions is similar to that inferred from linear response. These results emphasize the importance of contact breaking in determining the vibrational response in jammed packings that interact via purely repulsive linear spring as well as Hertzian potentials.

II. METHODS

We first prepared MS packings of frictionless disks using the successive-compression-and-decompression algorithm [8] at a given deviation in packing fraction above jamming onset $\Delta\phi = \phi - \phi_J$ for systems composed of $N = 32$ to 128 disks. We then performed molecular dynamics simulations at constant total energy E in a periodic square cell of N frictionless disks that interact via purely repulsive pair potentials:

$$\vec{F}_{ij} = \frac{\epsilon}{\sigma_{ij}} \left(1 - \frac{r_{ij}}{\sigma_{ij}}\right)^\alpha \Theta\left(1 - \frac{r_{ij}}{\sigma_{ij}}\right) \hat{r}_{ij} \quad (1)$$

where r_{ij} is the separation between particles i and j , $\hat{r}_{ij} = (x_{ij}\hat{x} + y_{ij}\hat{y})/\sqrt{x_{ij}^2 + y_{ij}^2}$ is a unit vector that points from particle j to i , $\Theta(1 - r_{ij}/\sigma_{ij})$ is the Heaviside step function that ensures that particles do not interact when they do not overlap, $\sigma_{ij} = (\sigma_i + \sigma_j)/2$, σ_i is the diameter of disk i , and $\epsilon = 1$ is the characteristic energy scale of the repulsive interaction. The power-law exponent α determines the form of the repulsive interactions, where $\alpha = 1$ (3/2) denotes the linear (Hertzian) spring interaction. We consider bidisperse mixtures with half large and half small particles and size ratio $d = 1.4$ to inhibit crystallization [9].

The linear vibrational response for MS packings (that interact via the pairwise forces in Eq. 1) can be obtained from the dynamical matrix [10]

$$K_{\alpha\beta} = \left. \frac{d^2V}{d\xi_\alpha d\xi_\beta} \right|_{\vec{\xi}=\vec{\xi}^0}, \quad (2)$$

where $V = \sum_{i,j=1}^N V(r_{ij})$ is the total potential energy, $\vec{F}_{ij} = -dV(r_{ij})/dr_{ij}\hat{r}_{ij}$, $\vec{\xi} = \{x_1, y_1, x_2, y_2, \dots, x_N, y_N\}$ give the positions of the disk centers, and K is evaluated at the MS packing, $\vec{\xi}^0$, which is a local minimum of V . K is a $2N \times 2N$ matrix that can be written in terms of the 2×2 block matrices

$$K'_{lm} = \begin{pmatrix} K_{x_l x_m} & K_{x_l y_m} \\ K_{y_l x_m} & K_{y_l y_m} \end{pmatrix}, \quad (3)$$

which in the $\Delta\phi \rightarrow 0$ limit reduces to

$$K'_{lm} \approx \alpha \left(\frac{\epsilon}{\sigma_{lm}^4} \right) \left(\frac{\sigma_{lm} F_{lm}}{\epsilon} \right)^{(\alpha-1)/\alpha} \begin{pmatrix} x_{lm}^2 & x_{lm} y_{lm} \\ x_{lm} y_{lm} & y_{lm}^2 \end{pmatrix}, \quad (4)$$

where $l \neq m$, $l, m = 1, \dots, N$ are the disk labels, $x_{lm} = x_l - x_m$, $y_{lm} = y_l - y_m$, and F_{lm} is the magnitude of the force \vec{F}_{lm} . The l th eigenvector of K , associated with eigenvalue k_l , is normalized so that $\sum_{i=1}^{2N} e_{li}^2 = 1$, where $\hat{e}_l = \{e_{lx_1}, e_{ly_1}, \dots, e_{lx_N}, e_{ly_N}\}$. The vibrational frequencies in the harmonic approximation are $\omega_l^d = \sqrt{k_l/m}$, where m is the mass of each disk.

We will compare the distribution of vibrational frequencies predicted from linear response to the vibrational response measured in molecular dynamics simulations. We vibrated each MS packing using two methods: 1) Perturb the static packing along one eigenmode l of the dynamical matrix by assigning the velocities $\vec{v}_i = \delta(E)\vec{e}_{li}$ to particle i , where \vec{e}_{li} gives the components of the l th eigenvector that correspond to particle i , $\delta(E) = \sqrt{2E/m}$, and E is the kinetic energy of the perturbation; and 2) Perturb the system along a superposition of the $2N - 2$ eigenmodes [11] by assigning $\vec{v}_i = \delta(E)\vec{e}_{\text{all}}$ where $\vec{e}_{\text{all}} = \frac{1}{\sqrt{2N-2}} \sum_{k=1}^{2N-2} \vec{e}_{ki}$.

For times $t > t_1 = 2\pi/\omega_1^d$ after the perturbation, where ω_1^d is the smallest dynamical matrix frequency, we measure the Fourier transform of the velocity autocorrelation function, which yields the distribution of vibrational frequencies

$$D(\omega^v) = \int_0^\infty dt \frac{\langle \vec{v}(t_0 + t) \cdot \vec{v}(t_0) \rangle}{\langle \vec{v}(t_0) \cdot \vec{v}(t_0) \rangle} e^{i\omega^v t}, \quad (5)$$

where $\langle \cdot \rangle$ indicates averages over all particles and time origins t_0 . We also measured the eigenvalue spectrum of the displacement correlation matrix [12]

$$C_{ij} = \langle (\xi_i - \xi_i^0)(\xi_j - \xi_j^0) \rangle, \quad (6)$$

where $i, j = 1 \dots 2N$ and the angle brackets indicate an average over time. The vibrational frequencies are obtained from the displacement correlation matrix eigenvalues, $\omega_k^c = \sqrt{T/c_k}$. The binned versions of the density of vibrational frequencies are given by $D(\omega^{c,d}) = [\mathcal{N}(\omega^{c,d} + \Delta\omega^{c,d}) - \mathcal{N}(\omega^{c,d})]/(\mathcal{N}(\infty)\Delta\omega^{c,d})$, where $\mathcal{N}(\omega)$ is the number of frequencies less than ω . $D(\omega^d)$, $D(\omega^v)$, and $D(\omega^c)$ are normalized so that $\int_0^\infty d\omega D(\omega) = 1$.

III. RESULTS

In linear response, the density of vibrational modes is similar for static packings that interact via purely repulsive linear and Hertzian spring interactions. In Fig. 1 (a), we show the density of vibrational modes $D(\bar{\omega}^d)$ obtained from the dynamical matrix for linear and Hertzian springs. Note that for Hertzian interactions, we considered scaled frequencies $\bar{\omega}^d = \omega^d / (\langle \omega^d \rangle_{\alpha=1.5} / \langle \omega^d \rangle_{\alpha=1})$ since the average frequency $\langle \omega^d \rangle_{\alpha=1.5} \sim (\Delta\phi)^{0.25}$ for Hertzian springs as

shown in Fig. 1 (c), whereas the average vibrational frequency for linear spring potentials $\langle \omega^d \rangle_{\alpha=1}$ is independent of $\Delta\phi$.

For packings near jamming onset that are isostatic, the pair force magnitudes for systems that interact via purely repulsive linear springs are proportional to those for Hertzian springs as shown in Fig. 1 (c). From Eqs. 3, this implies that the dynamical matrix elements depend on the force law, and thus the distribution of dynamical matrix frequencies varies with the force law for isostatic packings near jamming onset as emphasized in Fig. 1 (a).

In Fig. 1 (a), we show that the distribution of vibrational frequencies from the dynamical matrix develops a plateau that extends to successively lower frequencies as $\Delta\phi \rightarrow 0$ [13] for both linear and Hertzian springs (Eq. 1). For intermediate and large frequencies, the scaled $D(\bar{\omega}^d)$ does not depend strongly on $\Delta\phi$. However, we find that the weak peak in $D(\bar{\omega}^d)$ diminishes and $D(\bar{\omega}^d)$ extends to slightly larger frequencies for Hertzian compared to linear spring interactions.

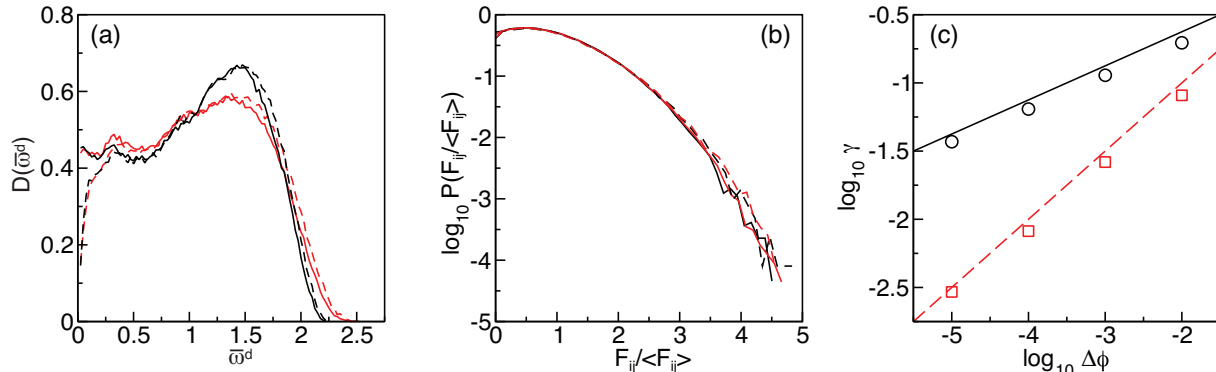


FIG. 1: (a) Density of vibrational modes $D(\bar{\omega}^d)$ from the dynamical matrix averaged over 800 static packings with $N = 128$ disks that interact via purely repulsive linear (black lines) and Hertzian (red lines) spring forces at $\Delta\phi = 10^{-5}$ (solid lines) and $\Delta\phi = 10^{-2}$ (dashed lines). The contact networks for the packings that interact via linear and Hertzian spring interactions are identical. We define $\bar{\omega}^d = \omega^d / (\langle \omega^d \rangle_{\alpha=1.5} / \langle \omega^d \rangle_{\alpha=1})$, where $\langle \omega^d \rangle_{\alpha}$ is the average vibration frequency for the force law in Eq. 1 with power-law exponent α . (b) Distribution of normalized pair force magnitudes $P(F_{ij} / \langle F_{ij} \rangle)$ for systems with purely repulsive linear and Hertzian spring interactions at $\Delta\phi = 10^{-5}$ and 10^{-2} using the same line types in (a). (c) Ratio of the average vibrational frequencies for purely repulsive Hertzian and linear spring interactions $\gamma_{\omega} = \langle \omega^d \rangle_{\alpha=1.5} / \langle \omega^d \rangle_{\alpha=1}$ (circles) and pair force magnitudes $\gamma_F = \langle F_{ij} \rangle_{\alpha=1.5} / \langle F_{ij} \rangle_{\alpha=1}$ (squares) versus the deviation in packing fraction from jamming onset $\Delta\phi$. The solid and dotted lines have slope 0.25 and 0.5, respectively.

In Fig. 2, we show the binned distribution of vibrational frequencies $D(\bar{\omega})$ from the dynamical matrix ($D(\bar{\omega}^d)$), displacement correlation matrix ($D(\bar{\omega}^c)$), and Fourier transform of the velocity autocorrelation function ($D(\bar{\omega}^v)$) for packings near jamming onset with linear and Hertzian spring interactions as a function of the perturbation energy. At sufficiently low perturbation energies, $D(\bar{\omega}^v)$ and $D(\bar{\omega}^c)$ both agree with $D(\bar{\omega}^d)$. For both linear and Hertzian spring interactions, $D(\bar{\omega}^v)$ and $D(\bar{\omega}^c)$ decay monotonically from a peak near $\bar{\omega} = 0$ at high perturbation energies that remove on average $\approx 50\%$ of the original contacts that were present at zero temperature. However, $D(\bar{\omega}^v)$ and $D(\bar{\omega}^c)$ do not have the same form at these energies; $D(\bar{\omega}^v)$ possesses a plateau at intermediate frequencies, whereas $D(\bar{\omega}^c)$ does not. In addition, for large perturbation energies, $D(\bar{\omega}^v)$ possesses a high frequency tail for purely repulsive Hertzian compared to linear spring interactions.

In Fig. 3, we show the measured vibrational response (frequency content of the Fourier transform of the velocity autocorrelation function) for packings near jamming onset with $N = 32$ that are perturbed along eigenmode 12 of the dynamical matrix over a range of perturbation energies. At perturbation energies $E < E_c$, where E_c is the energy above which a single contact breaks (Fig. 3 (a) and (c)), the vibrational response is confined to the original eigenfrequency of the perturbation ω_{12} for repulsive linear spring interactions (Fig. 3 (b)). In contrast, for packings with purely repulsive Hertzian spring interactions [14], the frequency response includes harmonics of the driving frequency ω_{12} even before contact breaking (Fig. 3 (d)), which arise from the factor $(1 - r_{ij}/\sigma_{ij})^{3/2}$ in the force law (Eq. 1).

For perturbation energies beyond which a single contact breaks, but before one contact is absent on average, $E_c < E < E_1$, the vibrational response is described mainly by a set of discrete frequencies. For both purely repulsive linear and Hertzian spring interactions, the discrete frequencies correspond to a combination of the eigenfrequencies of the dynamical matrix and low-frequency harmonics of the driving frequency (although the low-frequency harmonics possess a stronger signal for Hertzian spring interactions).

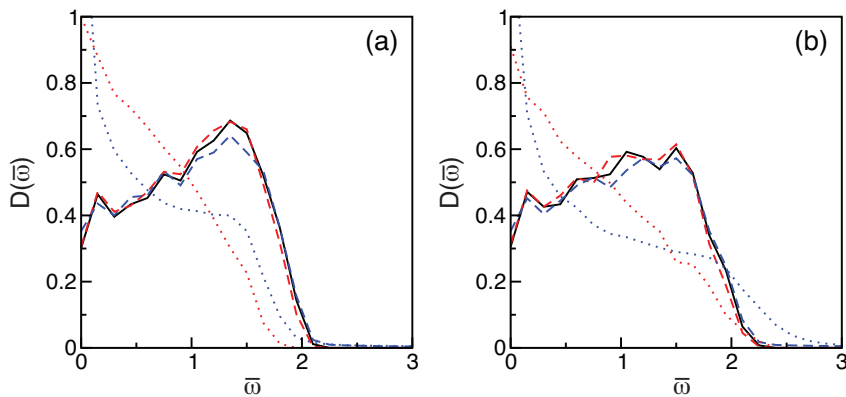


FIG. 2: The distribution of vibrational frequencies $D(\bar{\omega})$ for $N = 32$ bidisperse disk packings with $\Delta\phi = 10^{-4}$ using the dynamical matrix (black), displacement correlation matrix (red), and Fourier transform of the velocity autocorrelation function (blue) at perturbation energies where 0% (dashed) and 50% (dotted) of the contacts are missing on average from the zero-temperature configuration for purely repulsive (a) linear and (b) Hertzian spring interactions.

In the Appendix, we demonstrate for a simpler two degree-of-freedom system with double-sided Hertzian interactions that beats as well as harmonics of the driving frequency are present at large perturbation energies. However, in packings with single-sided interactions, contact breaking causes the vibrational response to become continuous before a significant number of harmonics and beats occur. We find in Fig. 3 (b) and (d) that for $E > E_1$ the vibrational response is described by nearly a uniform continuum of frequencies for packings with both purely repulsive linear and Hertzian spring interactions. Further, by comparing panels (a) and (b) (or (c) and (d)), the vibrational response develops significant weight at zero frequency when roughly 25% of the zero-temperature contacts are missing on average. These results emphasize that contact breaking (not the shape of the potential) dominates the nonlinear vibrational response for systems that interact via purely repulsive contact potentials [15].

How does the vibrational response depend on the nature of the perturbation applied to the static packing? In Fig. 4 (b) and (d), we show $D(\bar{\omega}^v)$ for the same packings studied in Fig. 3 after they are perturbed by a superposition of eigenmodes \bar{v}_{all} instead of by a single eigenmode of the dynamical matrix for both linear and Hertzian spring interactions. Because we chose the perturbation \bar{v}_{all} to include equal amounts of all dynamical matrix eigenmodes, at low perturbation energies $E \ll E_c$, $D(\bar{\omega}^v)$ is composed of the dynamical matrix eigenfrequencies with equal weights. At all perturbation energies $E < E_c$, $D(\bar{\omega}^v)$ exhibits peaks at the dynamical matrix eigenfrequencies with uniform weights for linear spring interactions. In contrast, there are slight differences in the weights at each of the dynamical matrix eigenfrequencies for Hertzian interactions for $E \lesssim E_c$ and for $E_c < E < E_1$ for both linear and Hertzian interactions. Similar to the behavior when perturbing along a single eigenmode, we find that the vibrational response includes a continuum of frequencies for $E \gtrsim E_1$. In addition, the density of vibrational modes becomes peaked near zero frequency when the average number of contacts drops to $\lesssim 25\%$ of its zero-temperature value. In this regime, the perturbation protocol does not affect the vibrational response.

IV. CONCLUSION

In summary, we performed molecular dynamics simulations to measure the vibrational response of static disk packings near jamming onset that interact via purely repulsive linear and Hertzian spring potentials. Instead of assuming linear response as in many previous studies (e.g. Refs. [13, 16]), we measured directly the vibrational frequencies from the Fourier transform of the velocity autocorrelation function and displacement correlation matrix. We find that although weak nonlinearities (e.g. the appearance of low-frequency harmonics of the driving frequency) occur at energies below contact breaking for packings that interact via Hertzian potentials, contact breaking dominates the vibrational response for energies $E > E_1$. The onset of nonlinearities from the shape of the Hertzian interaction potential occurs at a similar energy to that for contact breaking, however, contact breaking leads to much stronger nonlinearities in the vibrational response, e.g. the response spreads to a continuum of frequencies that are outside the range of the eigenfrequencies of the dynamical matrix for the static packing. Thus, we have shown that contact breaking gives rise to strongly nonharmonic response for systems with both purely repulsive linear and Hertzian interaction potentials.

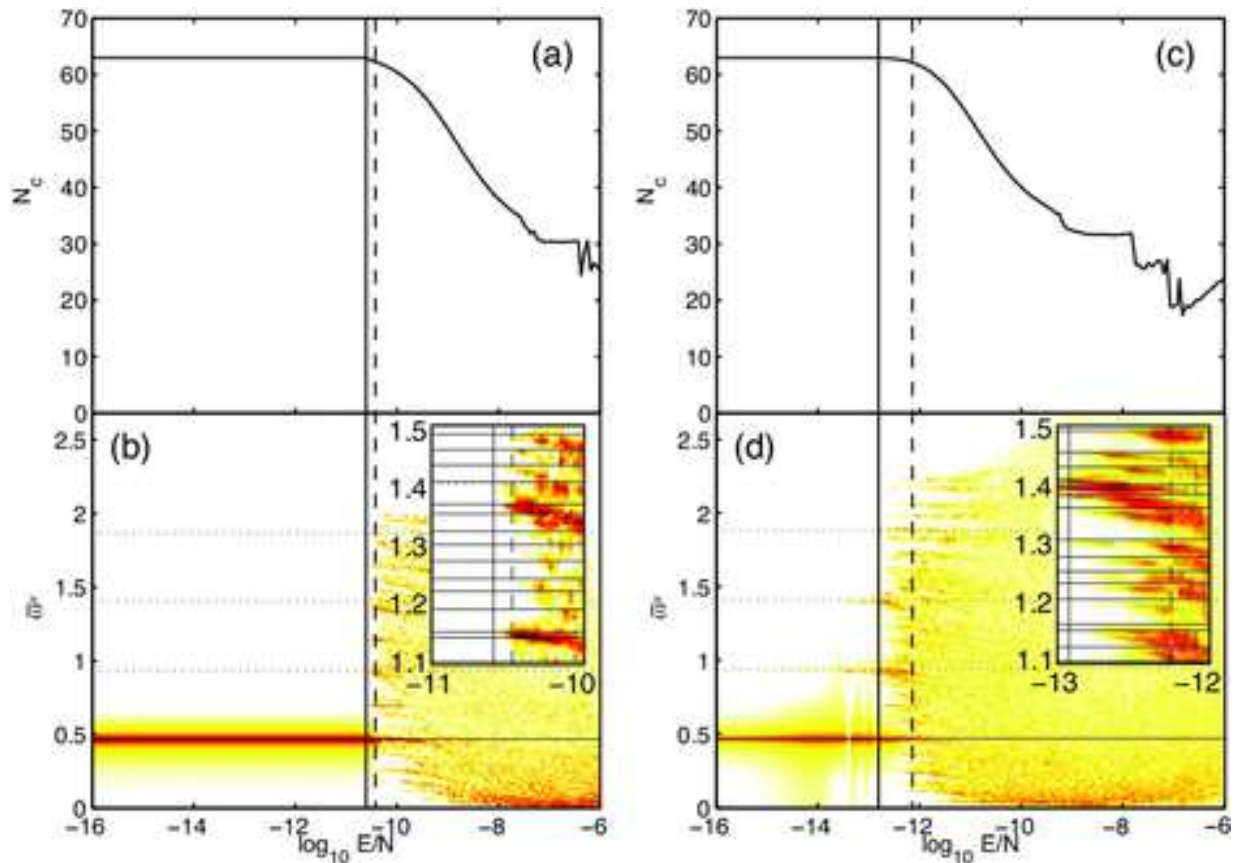


FIG. 3: Time-averaged number of contacts N_c ((a) and (c)) and color-scale plot of $\log_{10} D(\bar{\omega}^\nu)$ ((b) and (d)) for static packings of $N = 32$ bidisperse disks perturbed along a single eigenmode (mode 12) as a function of the perturbation energy E/N . At $E = 0$, the packing possesses the isostatic number of contacts $2N - 1 = 63$ contacts. In (b) and (d), the solid horizontal line represents the frequency of the driving frequency ω_{12} and the dotted horizontal lines indicate harmonics of the driving frequency, $2\omega_{12}$, $3\omega_{12}$, and $4\omega_{12}$. The vertical solid and dashed lines indicate the energies E_c above which the first contact breaks and E_1 above which there is on average one contact missing from the zero-temperature configuration. The inset shows a close-up of the region between E_c/N and E_1/N , where the solid horizontal lines give the dynamical matrix frequencies. The left (right) columns show the results for purely repulsive linear (Hertzian) spring interactions.

V. ACKNOWLEDGMENTS

We acknowledge support from NSF Grant No. CBET-0968013 (MS), DTRA Grant No. 1-10-1-0021 (CO), and Yale University (CS). This work also benefited from the facilities and staff of the Yale University Faculty of Arts and Sciences High Performance Computing Center and the NSF (Grant No. CNS-0821132) that in part funded acquisition of the computational facilities. We thank Bob Behringer for his kind mentorship and honest science over the past 25 years.

Appendix A: Simple Model

In this Appendix, we focus on a simple single-particle model to illustrate that contact breaking rather than nonlinearities that arise from the shape of the Hertzian potential dominates the vibrational response of static packings with purely repulsive Hertzian spring interactions. This model consists of a central, mobile disk that is confined between three fixed same-sized disks (Fig. 5 (a)). The system is compressed from the ‘just-touching’ configuration by growing all particle diameters by $\sigma' = (1 + \Delta)\sigma$, and then using energy minimization to find the new mechanically stable positions of the central disk $x'(\Delta)$ and $y'(\Delta)$. The disks interact via single-sided Hertzian spring forces (Eq. 1 with

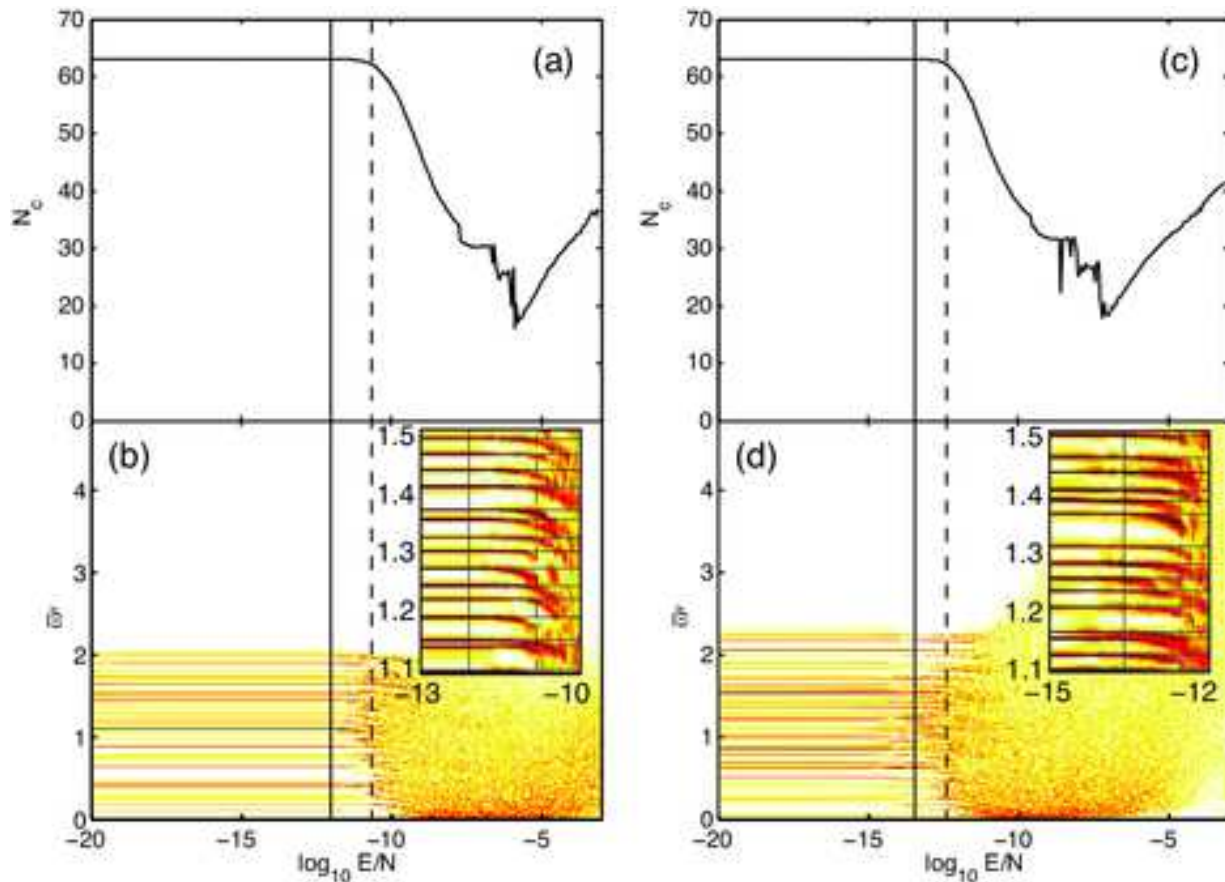


FIG. 4: Time-averaged number of contacts N_c ((a) and (c)) and color-scale plot of $\log_{10} D(\bar{\omega}^v)$ ((b) and (d)) for the same systems in Fig. 3 perturbed in a superposition of all eigenmodes of the dynamical matrix as a function of the perturbation energy E/N . The vertical solid and dashed lines indicate the energies E_c above which the first contact breaks and E_1 above which one contact on average is missing from the zero-temperature configuration. The insets are close-ups of the vibrational response for $E_c < E < E_1$. The left (right) columns show the results for purely repulsive linear (Hertzian) spring interactions.

$\alpha = 3/2$) or double-sided Hertzian spring forces (Eq. 1 with $\alpha = 3/2$ without the Heaviside step function)

$$\vec{F}_{ij} = \frac{\epsilon}{\sigma_{ij}} \left(1 - \frac{r_{ij}}{\sigma}\right)^{3/2} \hat{r}_{ij}, \quad (\text{A1})$$

for which all particles always interact with both repulsive ($r_{ij} < \sigma$) and attractive ($r_{ij} > \sigma$) forces. Studying this simple system allows us to clearly separate the eigenfrequencies of the dynamical matrix (linear response) from the additional frequencies in the vibrational response that are generated from the shape of the Hertzian potential and contact breaking (nonlinear response).

Figs. 5 (b) and (c) show the contours of the magnitude of the total force on the central disk for single- and double-sided Hertzian spring potentials, respectively. When the force magnitude contours are ellipsoidal and evenly spaced, the model system displays linear response. For both single- and double-sided Hertzian spring potentials, we find that deviations from linear response occur at energies near those that cause contact breaking (in single-sided systems). When contacts break in systems with single-sided interactions, the force magnitude contours become highly anisotropic and multi-lobed. In contrast, the model system with double-sided Hertzian spring interactions shows much weaker departures from linear response at large energies where contacts would break in systems with single-sided interactions.

In Fig. 6 (a)-(c), we show the vibrational response for the model system with double-sided Hertzian spring interactions obtained from the Fourier transform of the velocity autocorrelation function for several values of the energy of the central particle. At low energies much below contact breaking (in systems with single-sided interactions), only the two eigenfrequencies of the dynamical matrix are found in the vibrational response (Fig. 6 (a)). For energies close to and above contact breaking (in systems with single-sided interactions), the eigenfrequencies of the dynamical

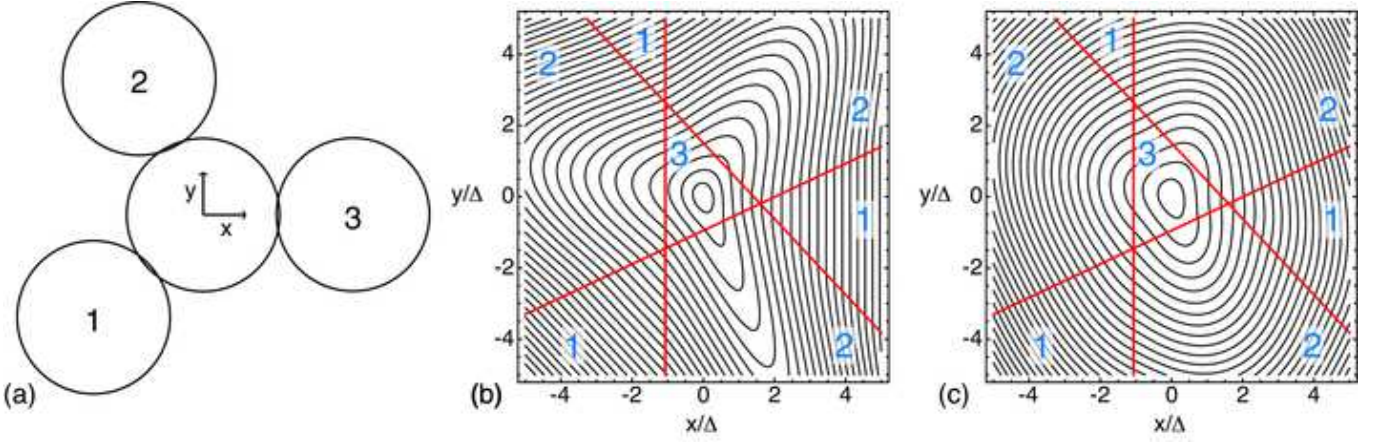


FIG. 5: Model system where a central mobile disk is confined by three same-sized fixed disks 1, 2, and 3 located at bond angles $\theta_{12} = 108^\circ$, $\theta_{23} = 115.2^\circ$, and $\theta_{31} = 136.8^\circ$. The initial amount of compression is $\Delta = 2 \times 10^{-2}$, and the disks interact via either single- or double-sided Hertzian spring potentials. (b) Contours of the magnitude of the total force on the central disk i from neighboring disks j , $|\sum_{j=1}^3 \vec{F}_{ij}|$, for single-sided Hertzian interactions at compression $\Delta = 10^{-4}$. The red lines indicate when the central particle loses or gains a contact with its neighbors, and the labels 1, 2, and 3 correspond to the number of contacts in each region bounded by the red lines. (c) Same as (b) except the disks interact via double-sided Hertzian spring interactions (Eq. A1).

matrix, low-frequency harmonics, and beats between them are found in the vibrational response (Fig. 6 (b) and (c)). In contrast, at energies above contact breaking in packings with single-sided Hertzian interactions the vibrational response shows a more continuous spectrum of frequencies spread well beyond the range of the original eigenfrequencies of the dynamical matrix. Previous work on Hertzian chains with double-sided interactions has shown that the vibrational response is periodic, but composed of non-sinusoidal nonlinear normal modes [17]. Further, beats occur because these modes are not orthogonal, and they mix with the eigenmodes of the dynamical matrix and their harmonics. A detailed analysis of nonlinear normal modes in packings with single-sided Hertzian spring potentials will be pursued in future studies.

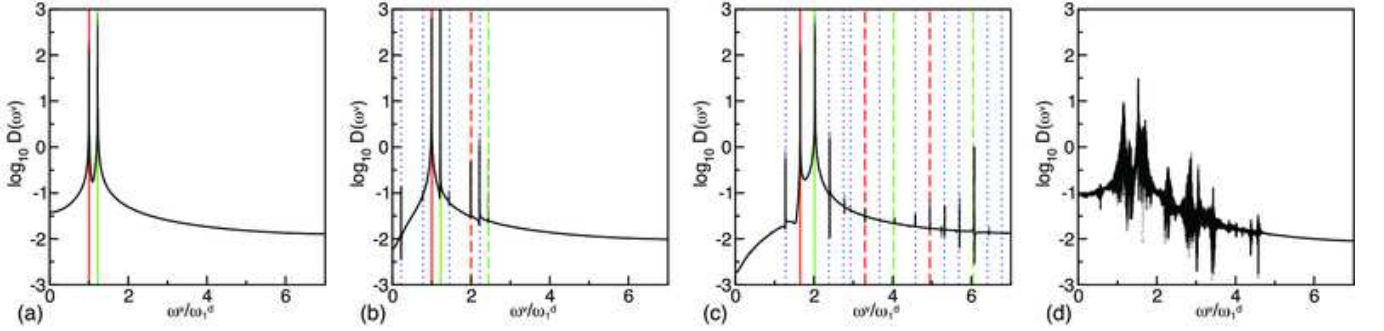


FIG. 6: Fourier transform of the velocity autocorrelation function $D(\omega^\nu)$ for the model system in Fig. 5 (a) with double-sided Hertzian spring interactions (Eq. A1) compressed by $\Delta = 10^{-4}$ and the central particle perturbed randomly at energies (a) $E/N = 10^{-16}$ (with an average number of contacts $\langle N_c \rangle = 3$), (b) $E/N = 3 \times 10^{-11}$ just below contact breaking for single-sided Hertzian spring interactions ($\langle N_c \rangle = 3$), and (c) $E/N = 10^{-7}$, which is far above the energy required to break a single contact on average for single-sided Hertzian spring potentials. In (d), we show the vibrational response for perturbation energy $E/N = 10^{-7}$ for the same systems in (a)-(c) except the disks interact via single-sided Hertzian spring potentials. The vertical solid lines correspond to the two dynamical matrix eigenfrequencies, the vertical dashed lines correspond to harmonics of the dynamical matrix eigenfrequencies, and the vertical dotted lines correspond to beats between the dynamical matrix eigenfrequencies and their harmonics. The frequencies ω^ν are normalized by ω_1^d , which is the smallest dynamical matrix eigenfrequency.

-
- [1] H. A. Makse, N. Gland, D. L. Johnson, and L. Schwartz, *Phys. Rev. E* **70** (2004) 061302.
 - [2] S. van den Wildenberg, M. van Hecke, and X. Jia, *Eur. Phys. Lett.* **101** (2013) 14004.
 - [3] N. Boechler, G. Theocharis, and C. Daraio, *Nature Materials* **10** (2011) 665.
 - [4] K. L. Johnson, *Contact Mechanics* (Cambridge University Press, Cambridge) 1985.
 - [5] V. Tournat, V. Zaitsev, V. Gusev, V. Nazarov, P. Béquin, and B. Castagnéde, *Phys. Rev. Lett.* **92** (2004) 085502.
 - [6] C. F. Schreck, T. Bertrand, C. S. O'Hern, and M. D. Shattuck, *Phys. Rev. Lett.* **107** (2011) 078301.
 - [7] T. Bertrand, C. F. Schreck, C. S. O'Hern, and M. D. Shattuck, unpublished (2013); xxx.lanl.gov/abs/1307.0440.
 - [8] G.-J. Gao, J. Blawdziewicz, and C. S. O'Hern, *Phys. Rev. E* **74** (2006) 061304.
 - [9] C. F. Schreck, C. S. O'Hern, and L. E. Silbert, *Phys. Rev. E* **84** (2011) 011305.
 - [10] A. Tanguy, J. P. Wittmer, F. Leonforte, and J.-L. Barrat, *Phys. Rev. B* **66** (2002) 174205.
 - [11] Two of the eigenvectors of the dynamical matrix correspond to uniform translations of the center of mass since we employ periodic boundary conditions in 2D.
 - [12] S. Henkes, C. Brito, and O. Dauchot, *Soft Matter* **8** (2012) 6092.
 - [13] C. S. O'Hern, L. E. Silbert, A. J. Liu, and S. R. Nagel, *Phys. Rev. E* **68** (2003) 011306.
 - [14] K. R. Jayaprakash, Y. Starosvetsky, A. F. Vakakis, M. Peeters, and G. Kerschen, *Nonlinear Dynamics* **63** (2011) 359.
 - [15] C. F. Schreck, T. Bertrand, C. S. O'Hern, and M. D. Shattuck, (unpublished) 2013; <http://xxx.lanl.gov/abs/1306.1961v1>
 - [16] L. Silbert, A. J. Liu, and S. R. Nagel, *Phys. Rev. E* **79** (2009) 021308.
 - [17] A. F. Vakakis, *Mechanical Systems and Signal Processing* **11** (1997) 3.